Path Planning Using Surface Shape and Ground Properties

Steven Martin
Queensland University of Technology
and CSIRO ICT Centre
Brisbane, Australia
steven.martin@qut.edu.au

Peter Corke
Queensland University of Technology
Brisbane, Australia
peter.corke@qut.edu.au

Abstract

This paper presents a path planning technique for ground vehicles that accounts for the dynamics of the vehicle, the topography of the terrain and the wheel/ground interaction properties such as friction. The first two properties can be estimated using well known sensors and techniques, but the third is not often estimated even though it has a significant effect on the motion of a high-speed vehicle. We introduce a technique which allows the estimation of wheel slip from which frictional parameters can be inferred. We present simulation results which show the importance of modelling topography and ground properties and experimental results which show how ground properties can be estimated along a 350m outdoor traverse.

Figure 1: QUT rOscar: the high-speed ground robot platform used in this work (length $\approx$ 50cm).

1 Introduction

Many approaches to robot path planning have been developed and have been used in real-world robot systems such as the DARPA Urban Challenge [13, 18]. However these well known approaches only solve the problem of generating a path that avoids obstacles or minimizes some objective function related to the cost of traversing particular regions of terrain. Planning dynamically feasible paths increases the dimensionality of the search space, requires modelling the vehicle dynamics rather than just the kinematics, and also presupposes knowledge of the vehicle's inertial and mass parameters, the suspension model, motor speed-torque curve, ground topography, and the frictional and dissipative phenomena where the tyre meets the ground (ground properties). This complexity means that the system dynamics is typically ignored, or grossly simplified, in the planning phase and accounted for by an online path-following controller at run time. However to achieve maximum performance it is important to model these dynamics, identify the parameters and account for them at planning time.

The contributions of this paper are computing dynamically feasible paths which the robot has the capability to follow. Firstly we investigate the significance of topography and ground properties for a simple simulation example where we use a Pseudospectral Optimal Control Solver for planning. Secondly we demonstrate the feasibility of online estimation of ground properties using the small-scale robot, shown in figure 1, for a 350m traverse we estimated the traction available.

1.1 Prior Work

A simple approach is to avoid regions which are difficult to traverse and a traversability metric can be defined to describe how difficult it is to traverse a region, and can be computed from properties such as slope, surface roughness, surface deformation, vehicle vibration, vehicle stability, friction, energy, completion time, colour or texture [2,8,9,16,17]. Some of these properties can be estimated in advance of arrival using, for example, laser scanner point clouds or camera imagery. Traversability metrics are useful as they provide a simple measure which can be used to optimise a global or local plan. Their disadvantage is that the properties are inferred rather than experienced.

Rather than avoid potentially difficult terrain the vehicle can make the best effort at run time to meet the plan. The simplest and most common approach to handling ground and

vehicle properties is to replan often. This is usually achieved using a two tier planner: global and local planning. A global planner searches the space to find a kinematically feasible path to the goal, perhaps taking some traversability data into account. Then a local planner accounts for vehicle dynamics, unknown obstacles and unmodelled properties and generates vehicle control inputs over a short look-ahead window. The local planner is run at a high rate to correct for discrepancies between the vehicle/terrain model and the real world. Such a structure is employed on the Willow Garage PR2 using the navigation software included in ROS middleware environment [12], and for outdoor robots such as [6], [7] and [14].

Rapid update of the local plan is essential to limit the divergence from the planned path, and this may limit the look ahead window of the planner and the complexity of the modelled vehicle dynamics. A consequence of limited look ahead is reduced ability to plan around large obstacles, while a simplistic vehicle model can produce infeasible or poor local paths.

The task of following a global or local path is a control problem known as path following which seeks to minimise the deviation of the vehicle from a given path. Typical state-of-the-art path following controllers use a dynamic vehicle model to predict the vehicles response and compute control inputs to minimise path deviation. This model is iteratively refined using the error in predicted trajectory, typically calculated from RTK GPS to compute unknown parameters, usually slip rates or cornering stiffness. Recent path followers have been shown to improve the vehicle's ability to accurately follow paths at high speeds of up to 8m/s. [10, 11]

The key assumption made by such approaches is that the terrain will be consistent, and recent developments have focussed on improving the rapid convergence at terrain transitions. [10] Another disadvantage of these algorithms is that parameters are not generalised for variations in vehicle speed, path radius of curvature or vehicle. This makes the use of such parameters in path planning difficult. Some initial investigations into generalisation of slip rates has been conducted by Marcovitz [15] however this has only been demonstrated on a limited data set and is unused in path planning.

2 Terrain Modelling

The effect of terrain is often ignored in path planning but accounting for surface topography and ground properties is important to optimise performance. Ground properties include characteristics such as friction, deformation and surface shear strength. We assume that properties are consistent for a known terrain type.

To investigate the advantages of accounting for terrain we constructed a simple optimisation-based path planner. We modelled the vehicle as a unicycle since it simplified the modelling of friction and is a commonly used approximation to a four wheel vehicle. We also assume that the ground properties are dominated by friction allowing dissipative phenomena, such as ground deformation, to be ignored.

A five-dimensional state space model is used to describe the unicycle.

$$X = \begin{bmatrix} x \\ y \\ v_x \\ v_y \\ \theta \end{bmatrix}, \quad \dot{X} = \begin{bmatrix} v_x \\ v_y \\ a_x \\ a_y \\ \dot{\theta} \end{bmatrix} \tag{1}$$

$$U = \begin{bmatrix} \zeta \\ \dot{\theta} \end{bmatrix} \tag{2}$$

The inputs are the fraction of motor torque ζ and the turn rate $\dot{\theta}$ with limits

$$0 < \zeta < 1 \tag{3}$$

$$-\frac{\pi}{4} < \dot{\theta} < \frac{\pi}{4} \text{rad/s} \tag{4}$$

Figure 2 shows the forces on the unicycle. F_W is the force due to torque on the wheel, F_T is the force due to lateral friction and S is the force due to slope.

The desired torque is,

$$T = T_{Max}\left(1 - \frac{{}^{V}V_X}{V_{Max}}\right)\zeta \tag{5}$$

where torque decreases linearly up to maximum velocity, V_{Max}. The longitudinal force on the wheel

$$\begin{aligned} F_W &= H\left(-(|{}^{V}V_X| - V_{Max})\right) \\ &\quad \left(H\left(F_r - \frac{T}{w_r}\right)\cdot F_r + H\left(\frac{T}{w_r} - F_r\right)\cdot\frac{T}{w_r}\right) \end{aligned} \tag{6}$$

is zero if the vehicle velocity exceeds V_{Max} and is limited by either motor torque or available friction, where friction is

$$F_r = \mu N \tag{7}$$

and N is the normal force.

The lateral force

$$F_T = -sgn\left({}^{V}V_Y\right) H\left(|{}^{V}V_Y|\right) F_r \tag{8}$$

always opposes the direction of motion and applies a maximum retarding force.

The acceleration of the vehicle in the world frame is

$$a_x = \frac{F_W\cos\theta + F_T\sin\theta + S_X}{m} \tag{9}$$

$$a_y = \frac{F_W\sin\theta + F_T\cos\theta + S_Y}{m} \tag{10}$$

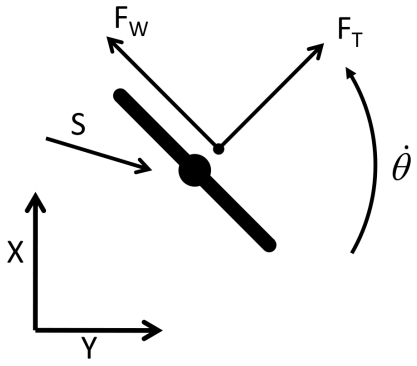

Figure 2: Forces on unicylce model. S is force in $X-Y$ plane due to slope and F_w & F_t are longitudinal and lateral wheel forces.

and the Heaviside, sign and absolute functions are implemented as smooth functions where $b = 0.01$.

$$H(x) = \frac{1+\tanh\left(\frac{x}{b}\right)}{2} \tag{11}$$

$$sgn(x) = \tanh\left(\frac{x}{b}\right) \tag{12}$$

$$|x| = \sqrt{x^2+b^2} \tag{13}$$

2.1 Path Planning

Finding a path through terrain was posed as an optimisation problem. We solved for minimum traversal time over a topography modelled by a mixture of Gaussians

$$Z = \sum_{i=1}^{n} h_i e^{-\frac{(X-x_i)^2+(Y-y_i)^2}{2\sigma^2}} \tag{14}$$

where $n = 4$ and the height of the peaks is given by $h = [2,1,1,4]$ centered at $[(-5,5),(-5,-5),(5,5),(1,-3)]$ and $\sigma = 2$.

For varying types of driving surface friction, μ, can range from $\mu \approx 0.10$ on ice up to $\mu \approx 0.85$ for dry asphalt [5]. To investigate the effect of wheel friction on a robot's ability to traverse the environment μ was modelled by

$$\mu = 0.8 \cdot |Y| + 0.2 \tag{15}$$

The maximum velocity of the vehicle was $V_{Max} = 5$m/s with a maximum applied torque $T_{Max} = 3$N.m. The mass of the vehicle $m = 3$kg and the wheel radius $w_r = 0.1$m. The vehicle was commanded to drive from a position of (-10,0) to (10,0) and with varying levels of model fidelity. If no topography or friction was given, the optimisation assumed a constant height of $Z = 0$m and a constant friction of $\mu = 0.4$.

The Pseudospectral Optimal Control Solver, PSOPT, [1] was used and was able to compute a single path taking ≈ 5 seconds, in 15-30 seconds on a HP Compaq 8000 Elite with Core2Duo E8600 processor and 4Gb of RAM. Figure 3 shows the optimised paths and table 1 shows the model fidelity and the planned time for execution, T_p.

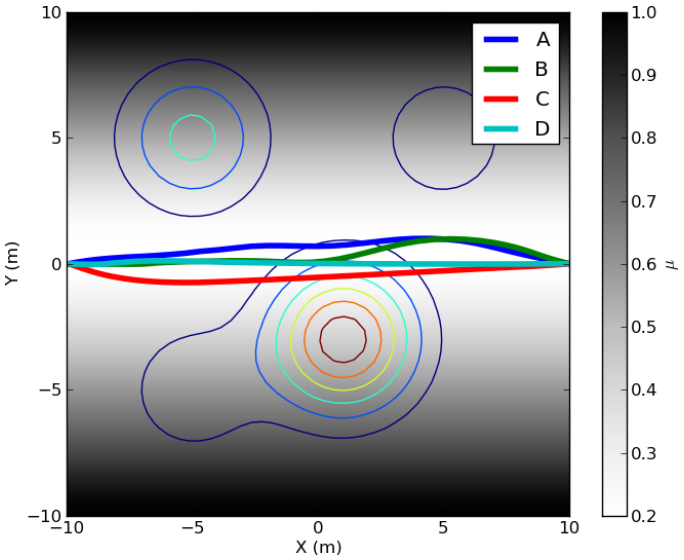

Figure 3: Paths A (red), B (blue), C (green) and D (light blue) are shown as as defined in table 1. The contours represent height of the terrain and surface shaded by friction.

Path D is a straight line from starting point to the goal, or shortest distance path, as there is no additional criteria to be optimised. Path C is biased in the Y-direction towards higher friction but as the optimisation has no knowledge of the topography the path fails to avoid the large peak centered at (1,-3).

Path B is optimised based on topography and the optimised trajectory for this path appears counter intuitive. The solution is optimal as the torque which can be applied by the motor is limited by vehicle velocity and there is no loss of energy over time. The vehicle accelerates up the edge of the peak then uses the gained potential energy to accelerate to a velocity greater than V_{Max}. Resulting in a trade off between motor torque, friction, time taken to climb the hill and the increased speed after the descent.

Path A accounts for both friction and topography and plans a route which avoids peaks and is biased towards higher wheel friction. The planned execution time is higher than paths B and D but the actual time to follow path A is expected to be lower due to the over estimation of friction in B and D. Path A also utilises the same stored energy effect resulting in a lower T_p than path C.

2.2 Simulation

A vehicle using a pure pursuit controller [3] was simulated to investigate the performance of a vehicle following these paths in environment with full fidelity. The controller outputs $\dot{\theta}^*$ based on the robot's pose and a look ahead distance of 1.0m. To perform the traversal in minimum time the simulated vehicle always accelerates at a maximum rate or ζ^*=1.

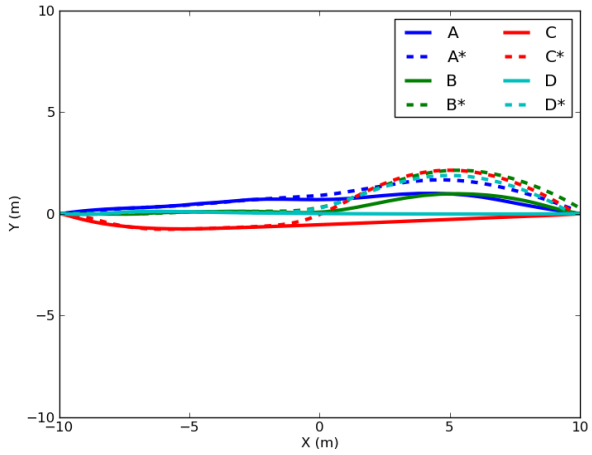

Figure 4: Paths A (red), B (blue), C (green) and D (light blue) show the planned (solid) and followed (dashed) path from simulation.

	Terrain Model		T_p	T_f	Avg Δ	Max Δ
	Friction	Topog.	(s)	(s)	(m)	(m)
A	✓	✓	4.58	4.20	0.22	0.73
B	x	✓	4.31	4.46	0.34	1.18
C	✓	x	5.14	4.49	0.71	2.45
D	x	x	4.35	4.39	0.52	1.91

Table 1: Comparison of planned, T_p, simulated, T_f, execution time and path deviation for planning with varying fidelity.

The look ahead distance was manually tuned and the performance of the simulated vehicle following each path is shown in figure 4 and table 1.

The simulation following path A reached the goal in the fastest time, T_f and also had the smallest average and maximum deviation from the path. As expected all other paths with lower model fidelity had longer completion times and larger deviations. Path C which accounted only for friction led to a worse result than path D which had no knowledge of the terrain. This is a special case but supports the need for accurate terrain information in order to optimise vehicle performance.

As expected Path A with the most complete model fidelity had the best performance indicating that friction and slope have a significant impact on vehicle dynamics. Arguably the performance of the simulated vehicle may be improved by a more sophisticated path following controller but improvements are expected for any controller in challenging terrain.

3 Mapping Ground Properties

Based on these results it is important to be able to determine the characteristics of the ground within an environment however, measuring these properties directly is difficult [4]. Traversability metrics have been used to infer these values using other measurable properties but these may not reflect the true ground properties. We have used an alternative approach of characterising terrain based on a vehicles response. This section details the development of a metric describing traction from sensor data using a small-scale mobile platform.

3.1 Vehicle

The vehicle used for the mapping is the QUT rOscar, shown in figure 1. It is based on a Traxxas Slash 1/8th scale RC car model, it is rear wheel drive and has an estimated top speed of 10m/s (36km/hr).

The car is equipped with a UTM-30LX Hokoyu laser scanner with a range of 30m at 40Hz, Xsens MTI-g AHRS system, Microstrain 3DM-GX2 and rear-wheel motor encoder. These sensors are connected via USB interface to a Gumstix Fire embedded linux system. The Gumstix is running Ubuntu 9.10 with ROS C Turtle middleware. All sensors are interfaced to ROS and the distributed functionality used to remotely log data from the vehicle.

3.2 Experiments

The vehicle's response to a step input was examined. It was accelerated from rest by a constant motor controller command. The vehicle then decelerated to a stop and the trial was repeated. The response to a step input was used as it was expected the excitation would produce a more deterministic signal than steady state operation. This was also influenced by the absence of accurate position information, such as RTK GPS.

The vehicles response to a step input was examined on three known ground types. The response of the vehicle on different ground types is clearly distinguishable for grass, gravel and tiled surfaces as shown by typical response curves in figure 5.

The acceleration is measured by the Microstrain 3DM-GX2, for each trial the gravity vector is calculated while at rest and the vehicles orientation is assumed to be constant for the trial duration. The net acceleration of the vehicle frame is calculated for each trial. The Microstrain 3DM-GX2 was used over the Xsens MTI-g as it was located at the vehicle centre of gravity. The MTI-g AHRS was primarily used to resolve measurement location from using GPS. This data, and all the data used for all further calculations has been filtered using a zero-order phase delay filter based on a third order Butterworth filter with a cut off frequency of 2.5Hz.

The calculation of ground properties, such as friction and shear strength, from acceleration is difficult due to the complexity of the tyre/ground interaction. Instead the term traction is used to refer to the net effect of these properties on vehicle motion.

The tiled surface is a high traction area indicated by a large acceleration peak and a slow rise in wheel velocity. The gravel is a low traction area and this can be seen in the low acceleration with a sharp initial rise in wheel velocity. The grass

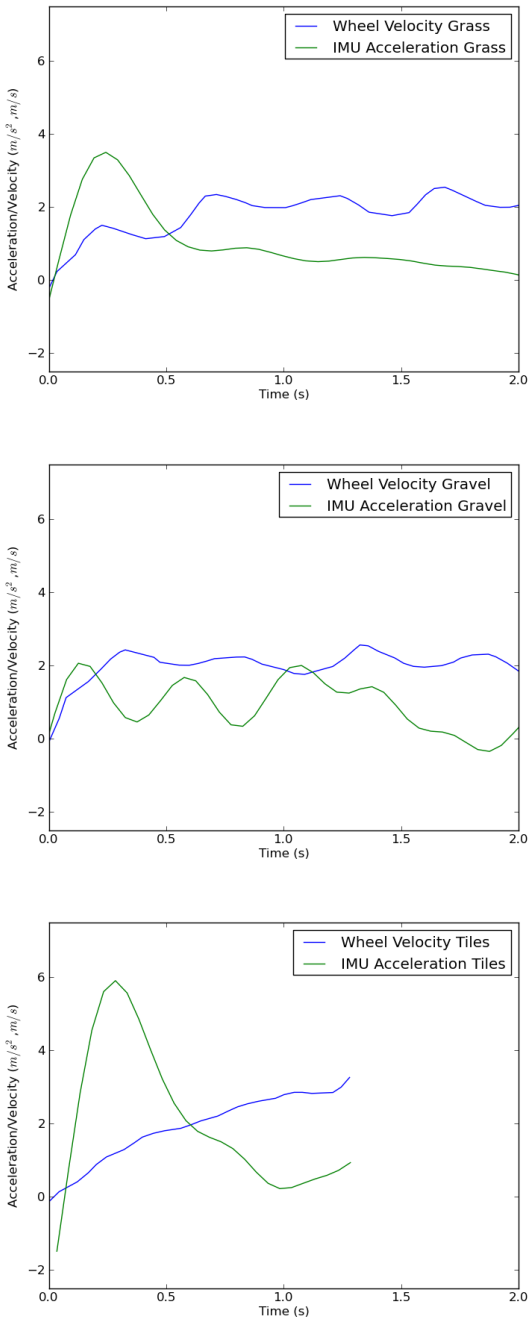

Figure 5: Typical wheel velocity and longitudinal acceleration responses of vehicle on grass, gravel and tiled surface.

is an intermediate surface showing characteristics of both surfaces. Figure 6, shows the acceleration of the vehicle for repeated trials on each surface. There is significant variation which is expected as no attempt was made to ensure identical paths were followed for repeated trials.

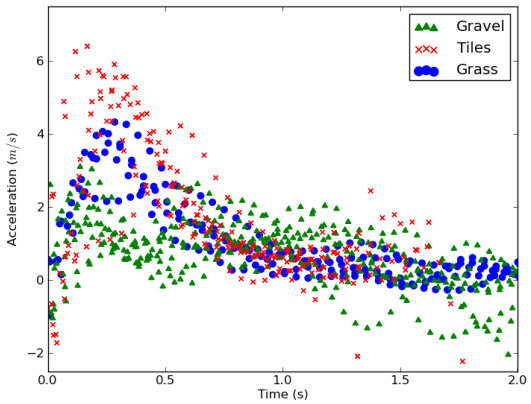

Figure 6: Filtered acceleration response for repeated trials on each surface.

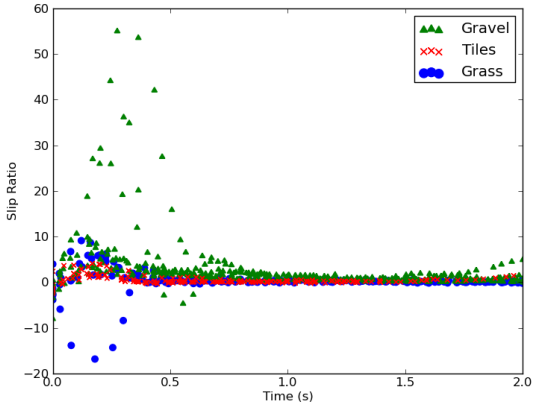

Figure 7: Filtered slip ratio for repeated trials on each surface.

3.3 Metric

A typical measure used to characterise the ground properties in path following algorithms is the longitudinal slip ratio. The slip ratio is calculated as shown,

$$\text{slip ratio} = \frac{\omega r - {}^{V}V_X}{{}^{V}V_X} \tag{16}$$

where ω is measured by the motor encoder and the longitudinal vehicle velocity, ${}^{V}V_X$ is obtained from integrated IMU acceleration. The definition of the slip ratio results in infinite slip when ${}^{V}V_X$=0.

As the vehicle is accelerating from rest this is problematic and makes the result highly susceptible to noise and drift from integrated acceleration, as can be seen in figure 7. Instead an alternate traction metric is proposed

$$T_R = \frac{\int_0^t {}^{V}V_X \, dt}{\int_0^t \omega r \, dt} \tag{17}$$

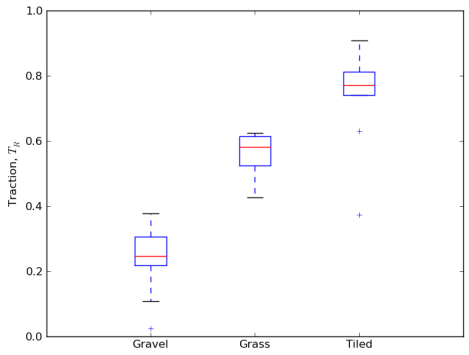

Figure 8: Traction metric as measured for multiple trials on known surfaces.

based on the ratio of longitudinal velocity to wheel velocity each integrated over window of t=0.6s for the rOscar vehicle. An index of 1 indicates high traction and an index of 0, low traction.

4 Results

The traversability metric was applied to the previous data and figure 8 shows the result for each trial classified by ground type. The metric shows a clear difference in traction.

Using the defined metric the rOscar platform was used to map the traction properties over an outdoor route. The vehicle was run in a 350m loop containing, concrete, grass, gravel and dirt surfaces. The vehicle used the same setup as the previous experiments with GPS used to localise each measurement.

The concrete area shown in figure 9 is clearly identified as the region with most available traction but no clear distinction can be made between the gravel/dirt and grass regions. This could be attributed to the slope of the terrain which is not accounted for in the metric, terrain variability or the vehicle reaching its limit of performance.

The off-road terrain which was traversed could be classified as very rough for a vehicle of this scale. This is shown by the blue samples in the gravel and dirt region, where $T_R \approx 0$ and the vehicle had to be assisted after becoming beached. We expect the difficulty of all off-road regions contributed to the variation of traction on the grass and gravel/dirt surfaces masking any distinction between the surfaces.

5 Conclusions

We have shown that surface shape and ground properties are important when planning high-speed paths and that ignoring these properties leads to sub-optimal plans which are difficult to follow at run time. We used a Pseudospectral Optimal Control Solver for planning based on a simplified, but dynamic, vehicle model, and the topography of the terrain and the wheel/ground interaction properties such as friction.

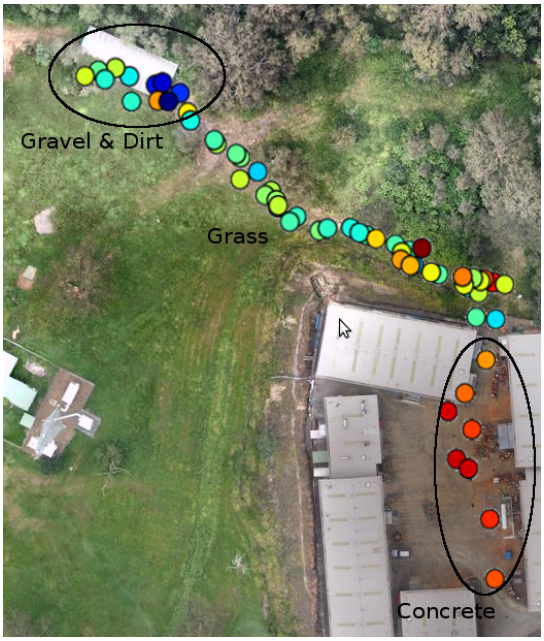

Figure 9: Traction plotted over test area, red indicates high traction and blue low traction regions. Samples take in gravel & dirt and concrete regions is shown, all other samples are assumed to be gathered on grass

Well known techniques can be applied to estimating the vehicle model parameters and well known sensors and techniques can be applied to topography estimation. We introduce a technique which allows the estimation of wheel slip from wheel speed and inertial sensing, and from which traction can be inferred. We presented experimental results for calculating the traction metric from a 350m outdoor traverse and were able to identify high traction areas.

We have a large program of ongoing work. The optimisation and simulation will be extended to include a tyre friction model to improve accuracy and the results of simulation and planning will be compared to real world experiments. Our experimental traverse included a significant slope which we did not explicitly account for in the ground property estimation. We will conduct a more comprehensive mapping of the operational area to provide the topography data required for optimised paths planned through the environment, and the improvement will be compared to other naive planning methods.

The metric we introduced captures only a very general measure of the ground properties. The interaction of the vehicle with the terrain is very complex and we will characterise a more complete description of the properties. The current metric focuses primarily on traction however other properties such as ground deformation and roughness will also have a significant impact on vehicle performance. We also need to explicitly account for uncertainty in the topography and ground property estimates and how this affects planning and run-time control, and how to infer ground properties from

laser or camera imagery.

We also plan to use visual odometry to determine the actual motion of the vehicle rather than rely on inertial/GPS estimation.

Acknowledgements

The authors are grateful for the technical and scholarship support from the CSIRO Autonomous Systems Lab.

References

[1] V.M. Becerra. Solving complex optimal control problems at no cost with PSOPT. In *Computer-Aided Control System Design (CACSD), 2010 IEEE International Symposium on*, pages 1391–1396. IEEE.

[2] C. Brooks, K. Iagnemma, and S. Dubowsky. Vibration-based terrain analysis for mobile robots. In *Robotics and Automation, 2005. ICRA 2005. Proceedings of the 2005 IEEE International Conference on*, pages 3415–3420. IEEE, 2005.

[3] R.C. Coulter. Implementation of the pure pursuit path tracking algorithm. 1992.

[4] P. Giguere and G. Dudek. Clustering sensor data for autonomous terrain identification using time-dependency. *Autonomous Robots*, 26(2):171–186, 2009.

[5] F. Gustafsson. Slip-based tire-road friction estimation* 1. *Automatica*, 33(6):1087–1099, 1997.

[6] Thomas M. Howard and Alonzo Kelly. Optimal rough terrain trajectory generation for wheeled mobile robots. *International Journal of Robotics Research*, 26(2):141 – 166, 2007.

[7] T.M. Howard, C.J. Green, and A. Kelly. State space sampling of feasible motions for high performance mobile robot navigation in highly constrained environments. In *Field and Service Robotics: Results of the 6 th International Conference(STAR: Springer Tracts in Advanced Robotics Series Volume 42)*, volume 42, pages 585–593. Springer, 2008.

[8] K. Iagnemma and S. Dubowsky. *Mobile Robots in Rough Terrain*. Springer, 2004.

[9] D. Kim, J. Sun, S.M. Oh, J.M. Rehg, and A. Bobick. Traversability classification using unsupervised on-line visual learning for outdoor robot navigation. In *Proc. of Intl Conf. on Robotics and Automation (ICRA). IEEE*. Citeseer, 2006.

[10] Roland Lenain, Benoit Thuilot, Christophe Cariou, and Philippe Martinet. Mixed kinematic and dynamic sideslip angle observer for acurate control of fast off-road mobile robots. *Journal of Field Robotics*, 27:181–196, 2009.

[11] Chang Boon Low and Danwei Wang. Maneuverability and path following control of wheeled mobile robot in the presence of wheel skidding and slipping. *Journal of Field Robotics*, 27:127–144, 2009.

[12] E. Marder-Eppstein, E. Berger, T. Foote, B. Gerkey, and K. Konolige. The office marathon: Robust navigation in an indoor office environment. In *Robotics and Automation (ICRA), 2010 IEEE International Conference on*, pages 300–307. IEEE, 2010.

[13] M. Montemerlo, J. Becker, S. Bhat, H. Dahlkamp, D. Dolgov, S. Ettinger, D. Haehnel, T. Hilden, G. Hoffmann, B. Huhnke, et al. Junior: The stanford entry in the urban challenge. *Journal of field Robotics*, 25(9):569–597, 2008.

[14] M. Pivtoraiko, I.A.D. Nesnas, and A. Kelly. Autonomous robot navigation using advanced motion primitives. In *Aerospace conference, 2009 IEEE*, pages 1–7. IEEE.

[15] Forrest Rogers-Marcovitz. On-line mobile robotic dynamic modeling using integrated perturbative dynamics. Master's thesis, Robotics Institute, Carnegie Mellon University, Pittsburgh, PA, May 2010.

[16] Zvi Shiller and Yu-Rwei Gwo. Dynamic motion planning of autonomous vehicles. *IEEE Transactions on Robotics and Automation*, 7:241–249, 1991.

[17] B. Sofman, J. Bagnell, A. Stentz, and N. Vandapel. Terrain classification from aerial data to support ground vehicle navigation. Technical report, Robotics Institute, Carnegie Mellon University, 2005.

[18] C. Urmson, J. Anhalt, D. Bagnell, C. Baker, R. Bittner, MN Clark, J. Dolan, D. Duggins, T. Galatali, C. Geyer, et al. Autonomous driving in urban environments: Boss and the urban challenge. *Journal of Field Robotics*, 25(8):425–466, 2008.